

Comparing Estimates of Wind Turbine Fatigue Loads using Time-Domain and Spectral Methods

by

Patrick Ragan and Lance Manuel

REPRINTED FROM

WIND ENGINEERING

VOLUME 31, No. 2, 2007

MULTI-SCIENCE PUBLISHING COMPANY
5 WATES WAY · BRENTWOOD · ESSEX CM15 9TB · UK
TEL: +44(0)1277 224632 · FAX: +44(0)1277 223453
E-MAIL: mscience@globalnet.co.uk · WEB SITE: www.multi-science.co.uk

Comparing Estimates of Wind Turbine Fatigue Loads using Time-Domain and Spectral Methods

Patrick Ragan and Lance Manuel*

Dept. of Civil, Architectural, and Environmental Engineering, University of Texas, Austin, TX 78712, USA

Emails <pragan@mail.utexas.edu>, *Corresponding Author <lmanuel@mail.utexas.edu>

ABSTRACT

Fatigue analysis for wind turbines is typically carried out in the time domain, using cycle counting techniques such as ASTM's Rainflow Cycle-Counting Algorithm. As an alternative, earlier workers investigated the feasibility of estimating wind turbine fatigue loads using spectral techniques such as Dirlik's method to estimate stress range probability distributions that are based on spectral moments of the load in question. The present paper re-examines this approach with a particular view to assessing its limitations and advantages in the context of modern, large-scale wind turbines and design methods. These relative advantages are considered in terms of accuracy, statistical reliability, and efficiency of calculation. Field data on loads from a utility-scale 1.5 MW turbine near Lamar, Colorado in the Colorado Green Wind Farm are analyzed here as a representative example. The results show that valuable and reliable information about tower loads can be obtained very efficiently. By contrast, the limitations of the Dirlik method are highlighted by poor results for edgewise blade loads.

NOMENCLATURE

f	=	frequency in Hertz
m	=	material exponent for fatigue
m_n	=	n^{th} spectral moment
$p(S)$	=	stress range probability density function
D	=	cumulative fatigue damage fraction
EFL	=	constant-amplitude equivalent fatigue load
K	=	material parameter for fatigue damage at failure
N	=	number of stress cycles
N_F	=	number of stress cycles at failure
P	=	peaks per second
P_s	=	power spectral density function for stress range, S
S	=	stress range
T	=	lifetime of structure
Z	=	normalized stress range

1. INTRODUCTION

The purpose of this study is to assess the viability of estimating fatigue loads on a wind turbine by using the power spectrum of the associated stress time series, rather than counting stress

ranges in the time series itself. This method, which we refer to as Dirlik's method¹, has the potential to be quite useful for designers because it allows computationally expensive steps of simulation and rainflow counting to be bypassed. Using more conventional time-domain methods, very many simulations may be required for the rarely occurring larger (and more important) stress cycles to be realized, and to obtain adequate resolution of the stress range histograms. On the other hand, the load power spectrum for a given stationary inflow condition may be estimated with less statistical uncertainty and can, in turn, be used as the basis for estimation of a stress range probability density function (PDF) in Dirlik's method. In some cases, a power spectrum for a turbine rotor or tower load can be reliably estimated directly from a single simulation of the inflow field, and the resulting stress range PDF could then be used to predict fatigue damage on the component immediately. When more typical time-domain methods are used, basing fatigue load estimates on a single time series simulation is unwise, because the largest and most influential stress cycles that are possible for the given wind (inflow) conditions would likely not have been realized in the selected short ten-minute segment. The ability to estimate fatigue damage with a minimum amount of data makes a method based on use of power spectra an attractive alternative for estimating fatigue loads.

Figure 1 shows a schematic of the two procedures that we will use to estimate fatigue damage in this study. The two fatigue damage estimates will be compared, and we will assess how accurately Dirlik's spectral method is able to predict fatigue damage.

Alternate Methods for Fatigue Load Estimation

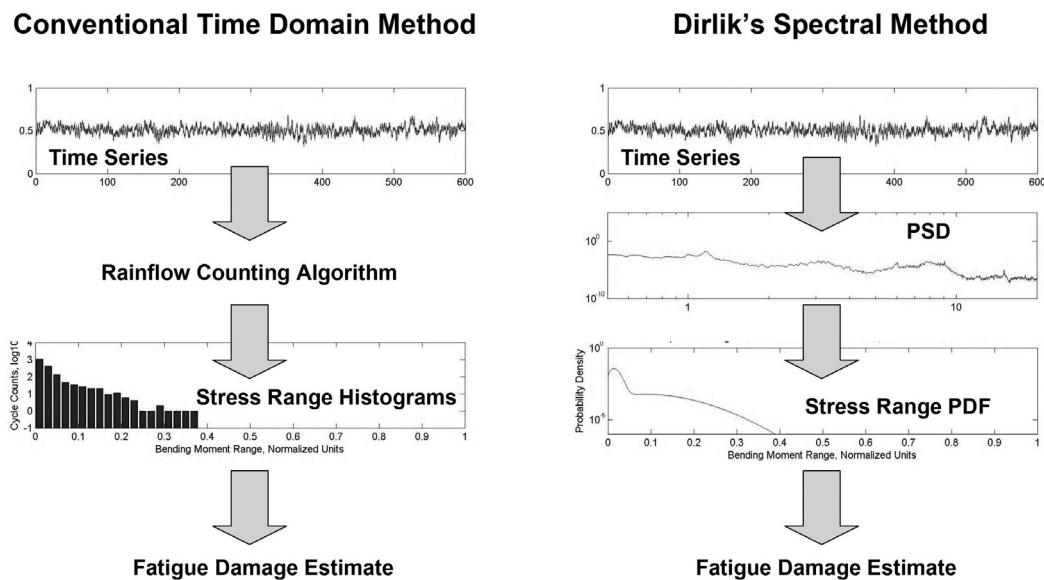


Figure 1. Comparison between procedures used in this study to estimate fatigue damage from field data.

2. EXPERIMENTAL DATASET

The subject of this study is a utility-scale 1.5MW wind turbine located at a Great Plains site near Lamar, Colorado (see Fig. 2). The turbine has a hub height of 80 meters and a rotor diameter of 70.5 meters. Approximately 17,000 ten-minute records were recorded over a period of roughly four months between September 2004 and January 2005 (Zayas et al²). A total of 67

channels at a 40 Hz sampling rate recorded various measurements of the turbine's inflow, control state, and structural response. For the purposes of this study, the following four measurements will be the subject of the fatigue load estimation:

1. *Edge Bending Moment*
(bending at the root of the blade, in the plane of the rotor)
2. *Flap Bending Moment*
(bending at the root of the blade, out of the plane of the rotor)
3. *Downwind Tower Moment*
(bending at the base of the tower, in the along-wind direction)
4. *Crosswind Tower Moment*
(bending at the base of the tower, in the cross-wind direction).

For various reasons, many of the original time series were unusable for our purposes. Of the original dataset of roughly 17,000 ten-minute records, a total of 2,485 were used in this study. Turbine load statistics are presented here as normalized values relative to the largest value observed during the measurement campaign for each of the four load types studied.



Figure 2. The Instrumented 1.5MW Wind Turbine.

3. CONVENTIONAL FATIGUE LOAD ESTIMATION IN THE TIME DOMAIN

3.1 Miner's Rule

A simple description of how fatigue damage accumulates on a structural component is given by Wohler's equation, which is recognized as the basis for fatigue analysis of wind turbines. Wohler's equation assumes that each cycle of a constant stress range amplitude, S , causes a particular amount of damage, and that damage increases linearly with the number of stress cycles applied, N , until it reaches a prescribed failure level. The damage induced in any single cycle is proportional to the stress range amplitude raised to the m^{th} power, where m is a material parameter which, in this study, is taken to be equal to 3 for the turbine tower (welded steel) and equal to 10 for the turbine blades (fiberglass composite). A second material parameter, K , is proportional to the number of cycles a material can withstand before failure. If we take N_F to be the number of cycles at failure, Wohler's equation may be expressed as:

$$N_F S^m = K \quad (1)$$

or

$$\log S = (\log K - \log N_F)/m \quad (2)$$

Equation (2) defines the familiar $S-N$ curve, which is linear on a log-log plot (see Fig. 3), and describes the failure zone as any $S-N$ pair that falls above the line. Alternatively, if N is any number of cycles before failure, we can modify equation (1) as follows:

$$D = \frac{NS^m}{K} \quad (3)$$

where the damage fraction, D , is a number between zero and unity; failure is reached when $D = 1$.

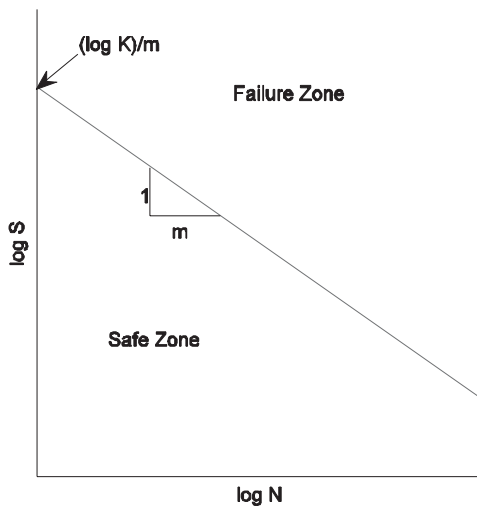


Figure 3. Representative $S-N$ fatigue curve.

3.2 Rainflow Counting for Variable Stress Cycle Amplitudes

A variable-amplitude cyclic stress time series may be decomposed into individual stress cycles using the Rainflow Cycle-Counting Algorithm³ and it is assumed that these individual cycles, S_i , may be superimposed upon one another. Now, N is the number of stress cycles that have been rainflow-counted and, in this study, N is taken to be the number of full cycles plus the

number of half-cycles weighted by a factor of 0.5. (See Reference 3 for definitions of the Rainflow-Counting Algorithm and other terminology including full and half cycles.) Using the computed S_i and N values extracted from the Rainflow-Counting Algorithm, Eq. (3) becomes:

$$D = \frac{\sum_{i=1}^N S_i^m}{K}, \quad (4)$$

which is referred to as Miner's sum.

It is sometimes useful to frame the concept of fatigue damage in terms of an *equivalent fatigue load*, which is the constant-amplitude stress range that would, over the same number of cycles, cause an equivalent amount of damage as the original variable-amplitude stress time series⁴. Using the following definition,

$$EFL = \left(\sum_{i=1}^N \frac{S_i^m}{N} \right)^{1/m} \quad (5)$$

it is then possible to rewrite Eq. (4) in the same manner as Eq. (3):

$$D = \frac{N(EFL)^m}{K} \quad (6)$$

4. DIRLIK'S METHOD

We now turn our attention to the problem of estimating fatigue damage in the frequency domain. We would like to avoid obtaining time series on loads from extensive simulation or field measurements that is typically followed by application of the Rainflow Cycle-Counting Algorithm, and instead be able to obtain equivalent information to cycle counts, such as a stress-range probability density function, directly from a power spectrum. If the stress process of interest were a narrow-band Gaussian process, then the PDF of the peaks of this process would be described by a Rayleigh distribution. Since each peak is associated with a trough of similar magnitude, the PDF of the stress ranges would also follow a Rayleigh distribution. However, most wind turbine load processes cannot be considered narrow-band, nor are they Gaussian in general, because of the presence of significant periodic components.

4.1 Formulation

Dirlik¹ proposed a method to estimate the probability density function of stress ranges that is intended to be applicable to both wide- and narrow-band processes. This method was developed by considering more than 60 different processes with power spectra of various shapes, computing their stress range distributions in the time domain via rainflow cycle counting, and fitting a general expression for the stress range PDF in terms of the 0th, 1st, 2nd, and 4th spectral moments. The formula for Dirlik's stress range PDF, which is a weighted combination of an exponential and two Rayleigh distributions, is reproduced below.

$$p(S) = \frac{\frac{D_1}{Q} e^{-Z/Q} + \frac{D_2 Z}{R^2} e^{-(Z^2/2R^2)} + D_2 Z e^{-Z^2/2}}{2\sqrt{m_0}}, \quad (7)$$

where Z is a normalized stress range,

$$Z = \frac{S}{2\sqrt{m_0}}, \quad (8)$$

m_n are the spectral moments,

$$m_n = \int_0^{\infty} f^n P_s(f) df, \quad (9)$$

A regularity factor, γ , representing the expected ratio of zero-crossings to peaks, is needed and is defined as follows:

$$\gamma = \frac{m_2}{\sqrt{m_0 m_4}}, \quad (10)$$

Also, a mean frequency is defined:

$$x_m = \frac{m_1}{m_0} \sqrt{\frac{m_2}{m_4}}, \quad (11)$$

Finally, empirical distribution weight factors appearing in Eq. (7) are defined as follows:

$$D_1 = \frac{2(x_m - \gamma^2)}{1 + \gamma^2}, \quad (12)$$

$$D_2 = \frac{1 - \gamma - D_1 + D_1^2}{1 - R}, \quad (13)$$

$$D_3 = 1 - D_1 - D_2, \quad (14)$$

$$Q = \frac{1.25(\gamma - D_3 - D_2 R)}{D_1}, \quad (15)$$

$$R = \frac{\gamma - x_m - D_1^2}{1 - \gamma - D_1 + D_1^2}. \quad (16)$$

Once the PDF, $p(S)$, has been estimated using this spectral approach, we may write a modified version of Eq. (5),

$$EFL = (E[S^m])^{1/m}, \quad (17)$$

where

$$E[S^m] = \int_0^{\infty} S^m p(S) dS \quad (18)$$

To predict the amount of accumulated damage, as Eq. (3) does, we also need to estimate the number of stress ranges, N , the process undergoes in time, T . Conveniently, the expected number of peaks per unit time, $E[P]$, may be related to the spectral moments:

$$E[P] = \sqrt{\frac{m_4}{m_2}} \quad (19)$$

and the expected number of cycles in T seconds is

$$E[N] = T \cdot E[P]. \quad (20)$$

Hence, directly analogous to Eq. (3), we have for the spectral method,

$$E[D] = \frac{E[N] \cdot E[S^m]}{K} = \frac{T}{K} E[P] \cdot E[S^m] \quad (21)$$

or, in terms of the equivalent fatigue load,

$$E[D] = \frac{E[N] \cdot (EFL)^m}{K} \quad (22)$$

4.2 Limitations

It should be noted that non-Gaussian processes and processes with large periodic components, such as those associated with the bending moments for the blades of a wind turbine, were not among the processes Dirlik considered in the development of the PDF given by Eq. (7)¹. Such processes are problematic to deal with in the frequency domain because the relative phasing (temporal correlation) of any large periodic components potentially becomes important in fatigue load estimates, but no phase information is retained in a power spectrum. An evaluation of the degree to which this effect undermines the utility of Dirlik's method for wind turbine applications is one of the motivations of the present study.

A previous application of Dirlik's method for wind turbine loads was carried out by Morgan and Tindal⁵, who used field data on flap bending moments from the MS1 turbine in Orkney, Scotland, and showed that the method performed rather well even in the presence of large periodic components. This study aims to re-examine similar wind turbine loads from a more modern utility-scale wind turbine as well as extend the scope to include edgewise blade loads and tower loads in two directions.

Finally, reference is made here to a recent publication by Sherratt, Bishop, and Dirlik⁶ for an up-to-date summary of spectral methods for fatigue analysis that is applicable to a range of different fields.

5. COMPARISON OF METHODS

5.1 Normalization of Results

For a given bending moment time series, we will compare the amount of damage predicted by Dirlik's method to that by the conventional time-domain method. One way to do this would be to simply compare the damage fractions calculated using each method in terms of the parameter, K , using for instance Eq. (6) for the conventional method and Eq. (22) for Dirlik's method. Alternatively, it is convenient to present results here in terms of 1000-cycle equivalent fatigue loads, which are the constant-amplitude load levels that would, over 1000 cycles, cause the same amount of damage as the variable-amplitude loads in a varying number of cycles. To convert an N -cycle equivalent fatigue load, EFL_N , into a 1000-cycle equivalent fatigue load, EFL_{1000} , associated with the same damage requires that we have:

$$\frac{N(EFL_N)^m}{K} = \frac{1000(EFL_{1000})^m}{K} \quad (23)$$

from which, we find that

$$EFL_{1000} = (N/1000)^{1/m} \cdot EFL_N \quad (24)$$

All the rainflow-counted results have been normalized in this manner. Dirlik's method results have been similarly normalized, but with the number of rainflow cycles, N , replaced by the expected number of cycles, $E[N]$, predicted from the spectral moments.

In summary, differences between the results calculated by each method will arise due to a combination of two possible effects:

1. the number of cycles predicted by Dirlik's method using Eq. (20) will in general be different from the number of rainflow-counted cycles; and
2. the equivalent fatigue load based on the Dirlik PDF of stress ranges (Eq. (17)), will be different from the equivalent fatigue load based on the rainflow-counted stress range histograms (Eq. (5)).

The normalization procedure described here allows differences in results from the two methods to be quantified by a single, physically interpretable value.

5.2 Time Series of Mathematical Interest

Before estimating fatigue loads using wind turbine field data on loads, we hope to gain insight into the strengths and weaknesses of Dirlik's method by comparing it to the conventional method for the following time series:

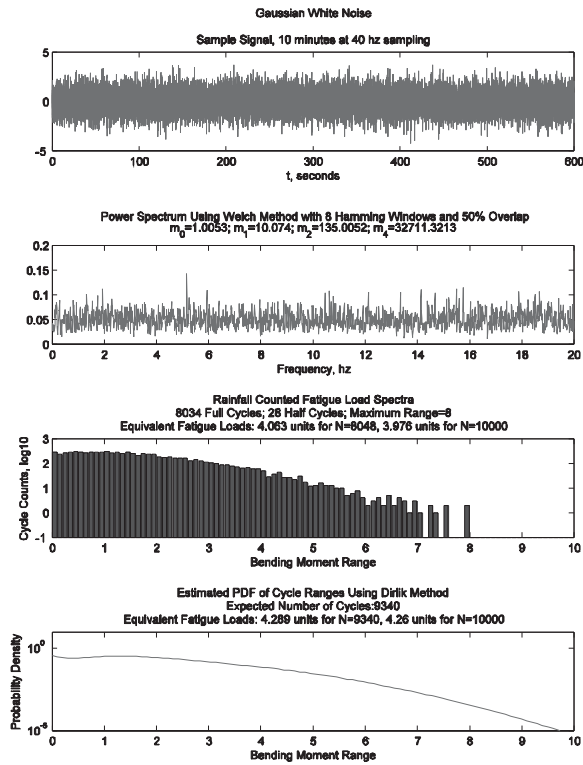
- Gaussian white noise: $\mu = 0, \sigma = 1$
- Gaussian white noise + sine wave: $x(t) = \cos[2\pi(.1)t] + \text{noise}, \mu_{\text{noise}} = 0, \sigma_{\text{noise}} = 0.25$
- Sum of sine waves, in phase: $x(t) = \cos[2\pi(.1)t] + 0.5\cos[2\pi(.3)t]$
- Sum of sine waves, out of phase: $x(t) = \cos[2\pi(.1)t] - 0.5\cos[2\pi(.3)t]$.

These four illustrative cases are summarized in Fig. 4. In each case, the original time series is plotted with its power spectrum estimate immediately below, the rainflow-counted stress histograms below that and, finally, the load PDF based on Dirlik's method at the bottom. The associated equivalent fatigue loads obtained for each method are also reported on the plots, both for the observed/expected number of cycles, N , as well as normalized values based on a constant number of cycles (1000, here). All calculations for these examples assume a material exponent, m , of 10.

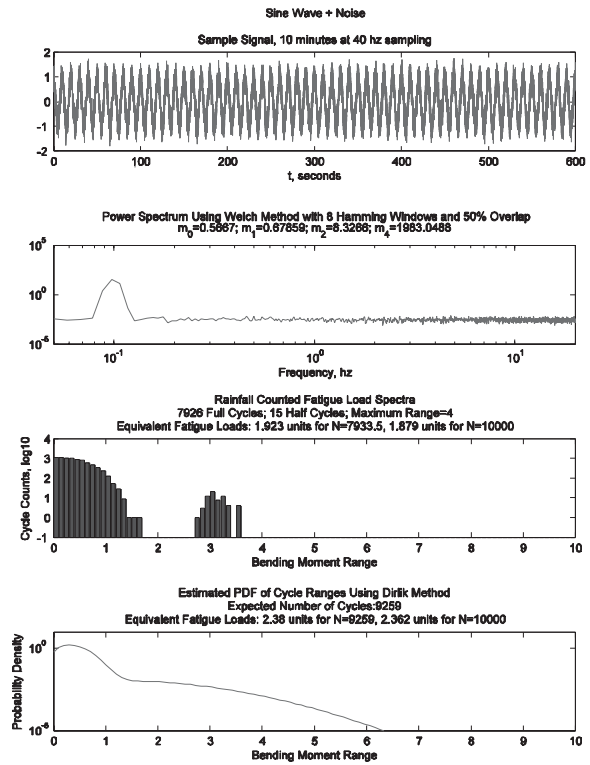
Estimation of the power spectra has been performed using the Welch method with 8 Hamming windows and 50% overlap. Some form of taper (Hamming or other) is recommended to reduce "leakage" from the spectral density near the large peaks in the spectrum to nearby regions.

A summary of the numerical results of the comparison between two methods is presented in Table 1. For both Gaussian white noise time series, the equivalent fatigue loads reported were normalized to a 10,000 cycles level, while for the "sum of sine waves" time series, the equivalent fatigue loads were normalized to 1000 cycles level. The percent error is the overestimation of Dirlik's method with respect to the conventional method.

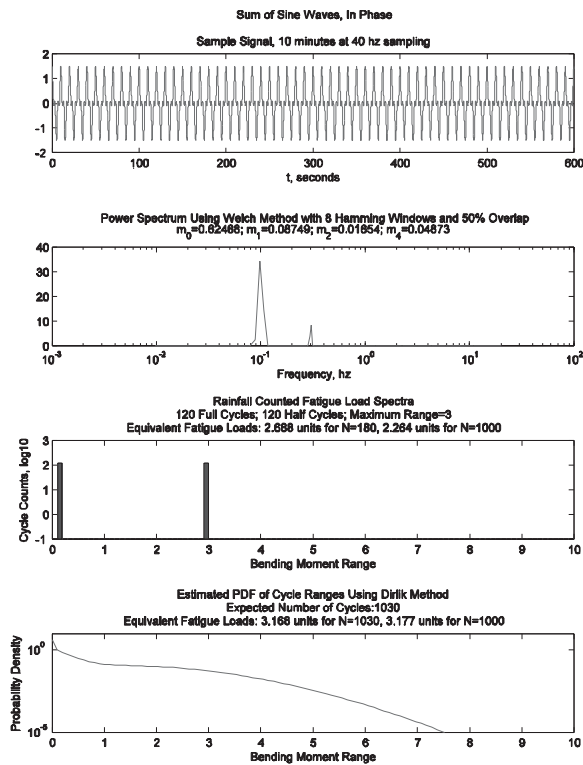
Form of Sample Time Series	Conventional Method			Dirlik's Method			
	N	EFL_N	$EFL_{10,000}$	$E[N]$	$EFLN$	$EFL_{10,000}$	% error
(a) Gaussian White Noise	8048	4.063	3.976	9340	4.289	4.260	7.1
(b) Sine Wave + Gaussian White Noise	7934	1.923	1.879	9259	2.380	2.362	25.7
(c) Sum of Sine Waves, In Phase	N	EFL_N	$EFL_{10,000}$	$E[N]$	$EFLN$	$EFL_{10,000}$	% error
(c) Sum of Sine Waves, In Phase	180	2.688	2.264	1030	3.168	3.177	40.3
(d) Sum of Sine Waves, Out of Phase	180	1.923	1.624	1050	3.207	3.222	98.4



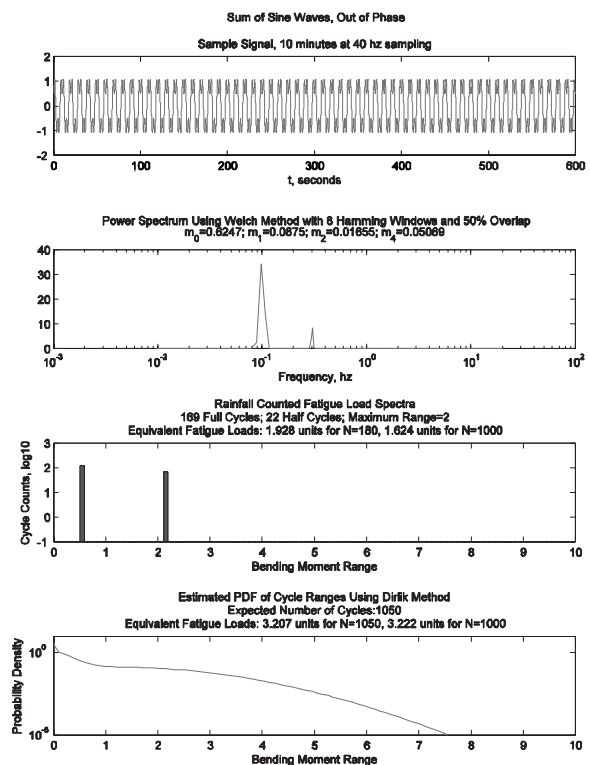
(a)



(b)



(c)



(d)

Figure 4. Comparison of Time-Domain and Spectral Methods for Four Illustrative Sample Time Series.

Figure 4(a) shows that Dirlik's method performs well for the case of white noise. The shape of the Dirlik PDF approximates the distribution of the histogram of rainflow counts quite closely, and the Dirlik EFL overestimates the 'true' EFL by only 7.1%.

For the case of a pure sine wave plus noise (Fig. 4(b)), the rainflow-counted stress range histogram has a bi-modal character, with higher stress ranges associated with the periodic component and lower stress ranges associated with the noise. The shape of the Dirlik PDF, however, does not exhibit this bimodal character. In fact, since Dirlik's method was not developed with the intention to model signals with large periodicities, it is in general unable to capture any bimodal character in the stress range density function. This well-understood limitation of Dirlik's method is one reason to be skeptical about its applicability to wind turbine loads, which often do exhibit large periodic components. On the other hand, it is interesting that the error even for this example (selected to exaggerate the degree of periodicity) in the Dirlik EFL estimate is not greater than around 26%; this indicates that even grossly incorrect estimation of the shape of the PDF does not necessarily correspond to an extremely inaccurate estimate of the EFL, even though the EFL is computed using the PDF.

The final two examples (Figs. 4(c) and 4(d)) are intended to demonstrate two things. The first is that when a time series is composed purely of sinusoids, the Dirlik PDF completely misrepresents the shape of the rainflow-counted stress range histograms. For reasons discussed above, this is not surprising nor is it terribly alarming because real signals from the field will rarely look like these. The second purpose for including these two examples is to demonstrate the inherent inability of Dirlik's method to recognize the effect that phase can have on fatigue damage. The rainflow-counted results show that when the two sine waves are in phase with each other, the equivalent fatigue load is 39% larger (2.264 vs. 1.624) than when they are out of phase. But since Dirlik's method is based on the power spectrum of the process, and the power spectrum only contains information on the amplitudes of the frequencies composing the process, and nothing about the phase, the method is unable to distinguish between the two signals. (The Dirlik estimate of the EFL should be theoretically identical regardless of phase; in actuality, small differences are seen in Figs. 4(c) and 4(d), but these can be explained by the imperfect precision associated with the spectrum estimation procedure.)

5.3 Time Series of Wind Turbine Loads from Field Data

The results from the preceding section suggest that in some cases Dirlik's method performs quite well, such as for a signal consisting completely of Gaussian white noise. On the other hand, as the signal becomes increasingly dominated by large periodic components, the accuracy of the Dirlik estimate decreases significantly. The relevant question, of course, is whether time series of wind turbine loads are close enough to Gaussian to be well modeled by Dirlik's method, or whether their periodic components are too large for Dirlik's method to be applicable.

Figure 5 shows a comparison of the time-domain and spectral methods applied to a single ten-minute time series on wind turbine loads obtained from the 17-19 m/s wind speed bin of the Lamar dataset, for each of the four load types of interest. A summary of the results for this sample file is presented in Table 2. Equivalent fatigue loads are in units of normalized moment, with each load type normalized by the largest moment observed for that load type over the course of the experimental campaign. (Note that each load type has been normalized by a different factor; hence, comparisons should be made only between the two methods of estimation, and not between the fatigue load estimates for the different load types.)

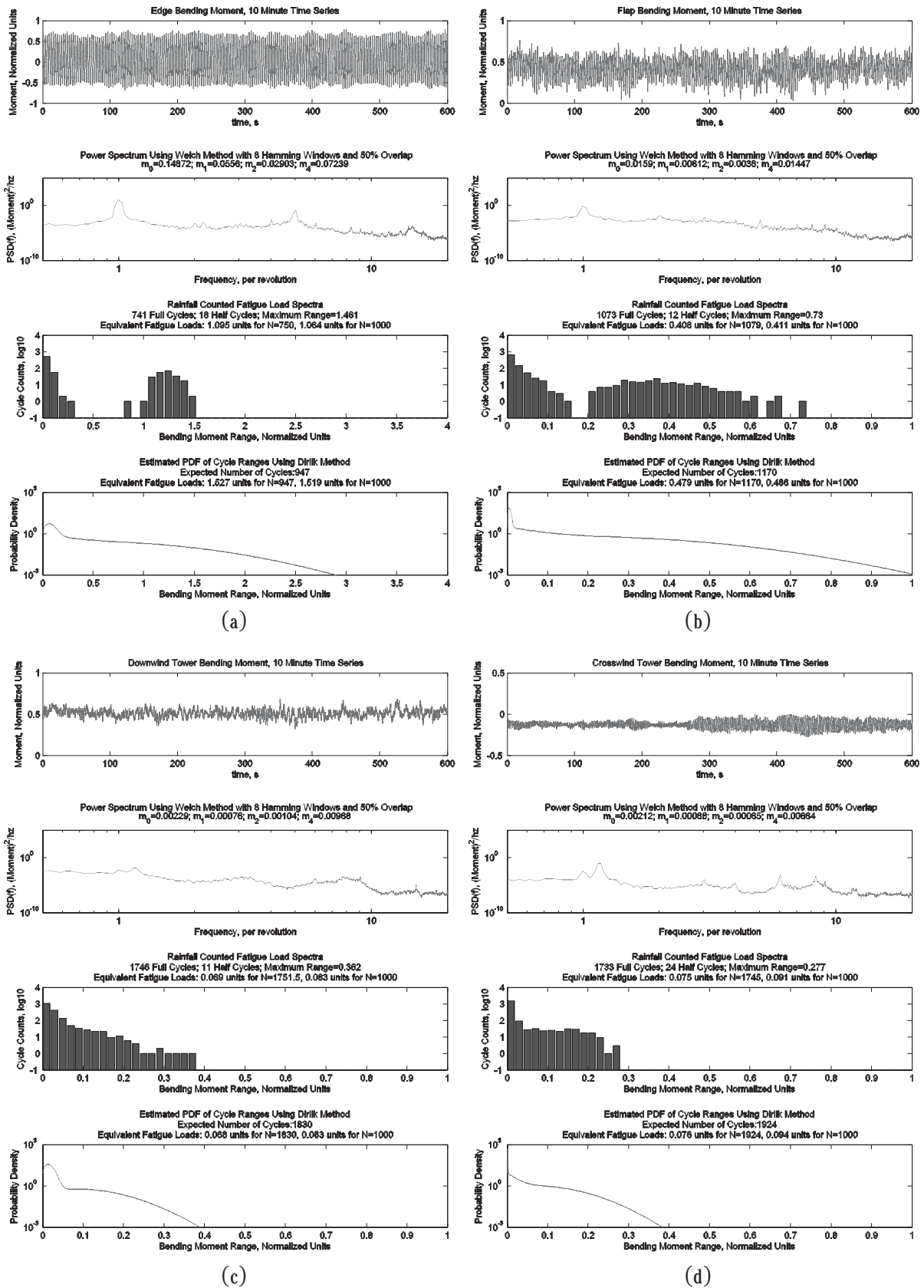


Figure 5. Comparison of Methods for Field Data on Sample Wind Turbine Loads (17-19 m/s bin).

Form of Sample Time Series	Conventional Method			Dirlik's Method			% error
	N	EFL_N	$EFL_{10,000}$	$E[N]$	EFL_N	$EFL_{10,000}$	
Blade Edge Bending Moment	750	1.095	1.064	947	1.527	1.519	42.8
Blade Flap Bending Moment	1079	0.408	0.411	1170	0.479	0.486	18.2
Downwind Tower Bending Moment	1752	0.069	0.083	1830	0.068	0.083	0.0
Crosswind Tower Bending Moment	1745	0.075	0.091	1924	0.076	0.094	3.3

Dirlik's method clearly performs far better for the tower bending loads than for blade bending loads, which is to be expected since tower loads have less dominant periodic components than the blade moments. For both tower load processes, the shape of the Dirlik PDF closely approximates that of the rainflow-counted stress range histogram (see Fig. 5) and, hence, the final 1000-cycle equivalent fatigue loads differ only slightly. For both blade load processes and especially for the edge bending moment, the Dirlik PDF is unable to capture the bimodal nature of the stress range histograms, and the equivalent fatigue load is overestimated quite noticeably. These results follow the trends presented in Fig. 4 and Table 1 pertaining to illustrative sample time series: for time series dominated by large periodic components, Dirlik's method overestimates the fatigue demand by a considerable margin.

5.4 Summary of Results for All Files

Calculations for the single ten-minute time series sample on wind turbine loads presented above were repeated for all of the 2,485 ten-minute files in our dataset. The scatter plots in Fig. 6 show the 1000-cycle equivalent fatigue loads from Dirlik's method versus those from the conventional method for all 2,485 records. (For instance, the ordered pair (1.064, 1.519), from Table 2, is one of the points included in the edge bending moment plot.) The diagonal dashed line in Fig. 6 is the locus of points for which the two methods would produce the same fatigue load estimate; points above this line represent instances where Dirlik's method overestimates the EFL relative to the conventional method; points below are cases where Dirlik's method estimate is below that from the conventional method. With the exception of edge bending moment, the points on these scatter plots follow the diagonal line reasonably closely, although they all show somewhat greater scatter above the line than below it.

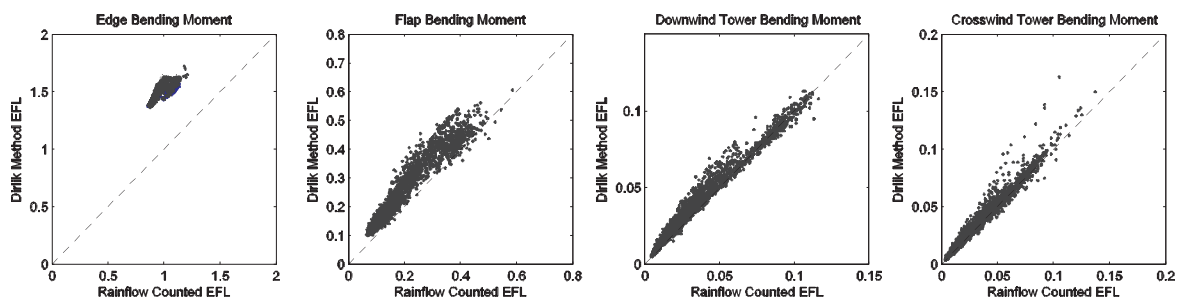


Figure 6. Conventional Method EFL vs. Dirlik EFL for the 2485 ten-minute files.

Figure 7 shows the distributions of the equivalent fatigue loads calculated using both methods. Note first that the shapes of the two distributions are quite similar, and second, that the accumulated fatigue damage over a ten-minute duration can be quite variable regardless of which method is employed to estimate it.

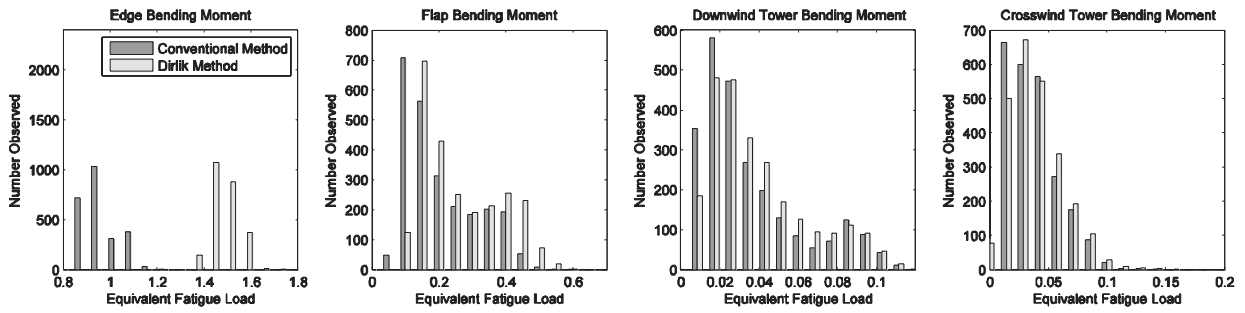


Figure 7. Distributions of Conventional Method EFL and Dirlik EFL for the 2485 ten-minute files.

In Fig. 8, the ratio of the Dirlik EFL estimate to the rainflow-counted EFL estimate has been calculated for the 2,485 files, and the distributions of this ratio are presented. If the two methods were consistently in close agreement, these distributions would be centered near unity with little spread. The actual distributions, however, all have mean values greater than unity, indicating a systematic overestimation of fatigue load on the part of Dirlik’s method—this is especially true for the edge bending loads. Moreover, sometimes, the dispersions about the mean can be great—e.g., for the blade flap loads.

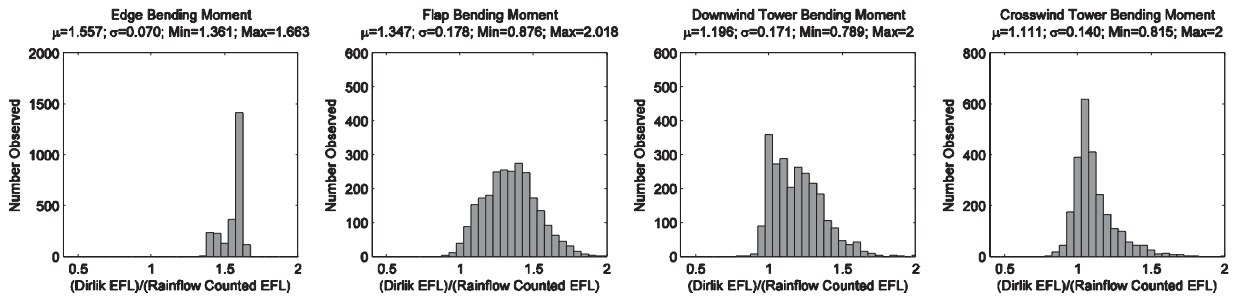


Figure 8. Distributions of Ratios of Dirlik EFL to Conventional Method EFL for the 2485 ten-minute files.

The root mean squared error (RMSE) presented in Table 3 is based on the difference between each calculated ratio and the target value of unity. Maximum and minimum values of the EFL ratio and mean values and upper and lower bounds of the 99% confidence intervals of the EFL ratio are also shown in Table 3.

Load	Minimum	.005 Fractile	Mean	.995 Fractile	Maximum	RMSE
Edge Blade Bending	1.361	1.380	1.557	1.649	1.663	0.561
Flap Blade Bending	0.876	0.968	1.347	1.842	2.018	0.390
Downwind Tower Bending	0.789	0.927	1.196	1.727	2.000	0.261
Crosswind Tower Bending	0.815	0.849	1.111	1.667	2.000	0.179

It is clear that Dirlik’s method fares better with the tower bending loads, which is to be expected given that Dirlik’s method’s main difficulty is in dealing with signals that have a large periodic component. Still, the method appears to overestimate the fatigue load for the vast majority of files (more on this shortly). For the edge bending moment process, which has the largest periodic component, Dirlik’s method performed the worst by several measures. The mean squared error is easily the worst of the four load types and, perhaps most tellingly, the smallest equivalent fatigue load predicted by Dirlik’s method is greater than the largest equivalent fatigue load predicted by the conventional method.

It should be noted that the poor performance of Dirlik's method for edge bending moment may not have such severe implications in design, since edge bending moment has the most consistent fatigue load by any measure (because it is dominated by the predictable periodic component). So while Dirlik's method is not recommended for estimating the fatigue associated with that load type, its fatigue demand may be reliably estimated with relatively few simulations in the time domain, whereas other load types would in general require many more simulations, and thus may be more efficiently evaluated for fatigue using Dirlik's method.

A note on the term 'overestimation' is in order here. Care must be taken in the interpretation of why Dirlik's method's fatigue loads estimates are generally seen to be higher than those from the conventional rainflow-counting method. There are potentially two factors working together to produce this effect. The first one, which we have been focusing on, is that there is a systematic bias on the part of Dirlik's method, which is a result of large periodic components in the wind turbine load time series that the method is not equipped (and was never developed) to handle. This is clearly the case for blade edge bending loads and, to a lesser extent, for blade flap bending loads. But one should also acknowledge that the conventional method might underestimate fatigue because the largest stress ranges possible under specified inflow conditions will usually not occur in the course of a single ten-minute sampling, and hence the stress range histogram will be missing the uppermost portion of its tail. This inability of short-term time domain simulations to reliably produce the largest possible stress cycles was, after all, one of the motivations for seeking a continuous PDF with Dirlik's (spectral) method in the first place. Hence, in this respect, it is not completely fair to say that Dirlik's method overestimates fatigue loads generally—this apparent overestimation could be in part due to an underestimation by the conventional method.

For this reason, conclusive recommendations cannot be made on the basis of the above results alone, which offer comparisons only for individual files. A fairer comparison can be made on a larger scale, by evaluating the overall amount of damage predicted by the two methods over a period of many days, when the stress range histograms have had a chance to "fill in." An example of a such a summary of results is presented in Table 4, both for the entire dataset (all files) as well as for individual wind speed bins. Specifically, the values shown are equivalent fatigue loads for all the files in a bin, normalized based on 1000 cycles per bin. (For example, if there are 200 files in a bin, then that bin's equivalent fatigue load has been normalized based on 200,000 cycles.)

Table 4. Overall Equivalent Fatigue Loads: Comparison between the Two Methods.

WS Bin	Blade Edge			Blade Flap			Downwind Tower			Crosswind Tower		
	Bending Moment			Bending Moment			Bending Moment			Bending Moment		
	Conv.	Dirlik	% error	Conv.	Dirlik	% error	Conv.	Dirlik	% error	Conv.	Dirlik	% error
All Files	0.985	1.498	52.1	0.344	0.394	14.3	0.052	0.054	4.2	0.047	0.051	7.2
5-7	0.896	1.436	60.2	0.208	0.275	32.2	0.020	0.026	29.0	0.017	0.021	21.5
7-9	0.913	1.449	58.7	0.208	0.288	38.6	0.027	0.034	24.4	0.031	0.036	14.5
9-11	0.940	1.495	59.1	0.250	0.340	35.9	0.036	0.044	22.1	0.046	0.052	13.1
11-13	0.973	1.553	59.6	0.250	0.346	38.3	0.035	0.040	15.8	0.041	0.043	6.7
13-15	1.016	1.557	53.3	0.325	0.424	30.4	0.044	0.047	7.0	0.043	0.045	4.9
15-17	1.069	1.565	46.4	0.346	0.414	19.6	0.065	0.066	1.6	0.057	0.059	4.6
17-19	1.088	1.542	41.8	0.415	0.465	12.1	0.084	0.085	0.9	0.070	0.072	3.6
19+	1.052	1.493	41.9	0.421	0.460	9.3	0.095	0.094	-1.1	0.081	0.085	5.8

The results in Table 4 follow similar trends to that in results previously discussed—i.e., Dirlik’s method overestimation is greatest for the edge bending moment and smallest for the two tower bending moments. In addition, note that in each case the error on the overall damage (Table 4) is lower than the average error on the damage predicted from individual files (from means in Table 3). For the reasons discussed above, this is to be expected, and these estimates from Table 4 should be considered a more accurate summary of the overall difference between the two methods’ predictions.

The bin-by-bin results in Table 4 also allow us to make the following interesting observation: agreement between the two methods is better for the higher wind speed bins than for the lower wind speed bins. The reason for this is that the character of the load processes changes markedly as wind speed increases. For lower wind speeds, the loads are more regular and, hence, more greatly influenced by the periodicity of the rotor rotation. Loads in higher wind speed bins display noisier and less periodic behavior. Since, as we have already seen when comparing the different load types, larger periodic components are associated with poorer performance of Dirlik’s method, it should be expected that there is also a difference in performance of Dirlik’s method at different wind speeds as is noted.

5.5 Recalculation of Results using Statistical Extrapolation of Rainflow-Counted Stress Ranges

Returning to the topic of potential underestimation of fatigue loads by the conventional method, it is not clear from the above results how much of the disparity between the two methods can be attributed to this effect alone, and how much is caused by a systematic overestimation of fatigue loads by Dirlik’s method. A more direct way to account for potential underestimation by the conventional method is to employ statistical extrapolation of the upper tail of rainflow-counted stress ranges. In this way the uppermost part of the stress range distribution tail, which in general will not have “filled in” over the course of a finite observation period, can be approximated by fitting a statistical distribution to some of the largest stress ranges that have been observed. Equivalent fatigue loads are then calculated using a hybrid approach based on the observed stress ranges that occurred below a certain threshold, and on statistically extrapolated stress ranges and associated probability densities above that threshold. This approach is recommended⁷ in Annex G of the IEC Standard 61400-1, Edition 3, and is demonstrated for simulated data in a study by Moriarty et al⁸.

The Moriarty et al study used a Weibull 3-parameter distribution fit to the top 1% of observed stress ranges from nine 10-minute simulations for each wind condition. We have used essentially the same method here to recalculate rainflow-counted equivalent fatigue loads for each of the 2,485 ten-minute files, but our extrapolations are based on the uppermost 5% of the tail, since our extrapolations are each based on only 10 minutes (rather than 90 minutes) of data. In general, extrapolation based on such a small amount of data as 10 minutes cannot be expected to be very reliable. In the aggregate, though, they at least serve our purpose of evaluating and adjusting for the potential of the conventional method to underestimate fatigue loads because of an incomplete upper tail of stress ranges.

Load	Minimum	.005 Fractile	Mean	.995 Fractile	Maximum	RMSE
Edge Blade Bending	1.362	1.380	1.557	1.649	1.664	0.561
Flap Blade Bending	0.668	0.842	1.285	1.753	1.930	0.341
Downwind Tower Bending	0.655	0.912	1.141	1.475	1.553	0.187
Crosswind Tower Bending	0.798	0.845	1.106	1.657	1.829	0.167

Table 5 summarizes recalculated EFL ratios using extrapolation, and these results may be compared with those in Table 3. With the exception of edge bending moment, mean ratios and RMS errors decrease in each case, indicating that underestimation on the part of the conventional method is indeed partly responsible for the apparent overestimation of Dirlik's method. For edge bending moment, the results have hardly changed because the largest stress ranges are associated with the relatively consistent periodic component of the signal; hence, the upper tail fills in after a relatively short amount of time and statistical extrapolation is unnecessary.

Table 6. Overall Equivalent Fatigue Loads, with and without Statistical Extrapolation.

WS Bin	Blade Edge			Blade Flap			Downwind Tower			Crosswind Tower		
	Bending Moment			Bending Moment			Bending Moment			Bending Moment		
	Conv.	Dirlik	% error	Conv.	Dirlik	% error	Conv.	Dirlik	% error	Conv.	Dirlik	% error
w/o extrap.	0.9847	1.4981	52.1	0.3444	0.3937	14.3	0.0516	0.0537	4.2	0.0474	0.0508	7.2
w/ extrap.	0.9845	1.4981	52.2	0.3594	0.3937	9.6	0.0518	0.0537	3.8	0.0473	0.0508	7.2

Recalculated versions of the overall equivalent fatigue loads (after extrapolation) are presented in Table 6, and may be compared with the prior results from the top line of Table 4. For flap bending moment and downwind tower bending moment, there is again some improvement or reduction in the Dirlik's method's error, but the differences are not dramatic, and there are no appreciable differences for edge bending moment and crosswind tower bending moment. Our conclusion, then, is that some underestimation of fatigue loads is possible when the conventional rainflow-counting method is used without statistical extrapolation of stress ranges; however, systematic overestimation of fatigue loads by Dirlik's method is in general a far more significant contributor to discrepancies between the two approaches. The degree of overestimation by Dirlik's method, of course, varies greatly between different load types and wind speeds as has been discussed at great length in previous sections.

6. CONCLUSIONS

Equivalent fatigue loads for a utility-scale wind turbine were estimated by two independent methods using field data consisting of 2,485 ten-minute time series of blade and tower bending moments. A comparison of results from the two methods suggests that Dirlik's method (a spectral approach) is a promising option for predicting fatigue loads for some, but not all wind turbine component loads.

In particular, our study showed that Dirlik estimates of fatigue load

- perform very well for tower bending moments, which exhibit only slight periodic character,
- perform moderately well for flap bending moment,
- perform very poorly for edge bending moment, which has a very large periodic component,
- perform better under windier and more turbulent conditions,
- are almost always more conservative than corresponding rainflow-counted fatigue load estimates.

Additional studies are necessary to conclusively evaluate the potential of Dirlik's method

for use in fatigue design of wind turbines. In particular, a simulation study would be very helpful. We hypothesize that for a simulated inflow field with a given mean hub-height wind speed and associated turbulence spectrum, spectral moments of structural loads on wind turbine components are likely to be quite stable, which would imply that the Dirlik PDF and associated fatigue damage could be estimated easily (on the basis of a few—say, m —ten-minute inflow turbulence simulations). These fatigue predictions should be compared with the results of rainflow-counted stress cycles over a very large number (say, n) of simulated load time series, all of which are generated using inflow fields with the same mean wind speed and turbulence target spectra. A reasonably close match between the fatigue load predictions from the two methods would indicate that estimates from Dirlik's method based on the m time series are of comparable quality to those based on the n time series using the conventional method, thus establishing the advantage in efficiency of the spectral approach, as long as m is much smaller than n . Such a comparison was not possible with the field data employed here because of the highly variable nature of the inflow.

Dirlik's method has the advantage of conveniently relying on spectral information that is easier to estimate than load histograms from limited data. The results of this study show that the method works very well in some cases, but rather poorly in others; as such, it may not always be the best choice for design validation. However, design validation is not the only realm of application. For tasks such as design optimization or sensitivity analysis, where the influence of a large number of design variants on some limiting aspect of the design needs to be found, a spectral method such as this one can provide a very useful tool.

ACKNOWLEDGMENTS

The authors gratefully acknowledge the financial support provided by Contract No. 30914 from Sandia National Laboratories and by a CAREER Award (No. CMS-0449128) from the National Science Foundation. They also are pleased to acknowledge useful discussions with Herb Sutherland, Paul Veers, and Jose Zayas at Sandia during the course of this work.

REFERENCES

- [1] Dirlik, T., "*Applications of Computers in Fatigue Analysis*," PhD Dissertation, University of Warwick, England, 1985.
- [2] Zayas, J. R., Sutherland, H. J., and Patton, T. C., "*Continuous Long-Term Test Program on a Utility-Scale Wind Turbine*," *Proceedings of the ASME Wind Energy Symposium*, AIAA, Reno, NV, 2006.
- [3] ASTM, "*Standard Practices for Cycle Counting in Fatigue Analysis*," American Society for Testing and Materials Standards, E1049-85, 1985.
- [4] Sutherland, H.J., "*On the Fatigue Analysis of Wind Turbines*," Sandia National Laboratories, SAND99-0089, 1999.
- [5] Morgan, C.A., and Tindal, A.J., "*Further Analysis of the Orkney MS-1 Data*," *Proceedings of the BWEA Conference*, pp. 325-330, 1990.
- [6] Sherratt, F, Bishop, N, and Dirlik, T., "*Predicting fatigue life from frequency-domain data: current methods*," *Journal of the Engineering Integrity Society*, September 2005.
- [7] IEC 61400-1 Ed. 3, *Wind Turbines – Part 1: Design Requirements*, International Electrotechnical Commission, IEC, 2005.
- [8] Moriarty, P.J., Holley, W.E., and Butterfield, S.P., "*Extrapolation of Extreme and Fatigue Loads using Probabilistic Methods*," NREL/TP-500-34421, 2004.

